

Effect of Sintering Temperature on the Phase Formation and Superconducting Properties of $\text{Bi}_{1.6}\text{Pb}_{0.4}\text{Sr}_2\text{Ca}_2\text{Cu}_3\text{O}_{10}$ Ceramics Synthesised via Co-Precipitation

Nurhidayah Mohd Hapipi¹, Soo Kien Chen^{1,2*}, Mohd Mustafa Awang Kechik¹, Kean Pah Lim¹, Abdul Halim Shaari¹, Nor Atikah Baharuddin¹, Nurul Auni Khalid¹, Muhammad Kashfi Shabdin¹, Kar Ban Tan³, Oon Jew Lee⁴

¹ Department of Physics, Faculty of Science, Universiti Putra Malaysia, 43400 UPM Serdang, Selangor, Malaysia

² Institute of Nanoscience and Nanotechnology (ION2), Universiti Putra Malaysia, 43400 UPM Serdang, Selangor, Malaysia

³ Department of Chemistry, Faculty of Science, Universiti Putra Malaysia, 43400 UPM Serdang, Selangor, Malaysia

⁴ Faculty of Science and Marine Environment, Universiti Malaysia Terengganu, 21030 Kuala Nerus, Terengganu, Malaysia

Received: May 30, 2025

Revised: August 7, 2025

Accepted: August 25, 2025

Published: August 31, 2025

Corresponding Author:

Soo Kien Chen

chensk@upm.edu.my

DOI:

© 2025 The Authors. This open access article is distributed under a (CC-BY License)



Abstract: In this work, (Bi, Pb)-2223 superconducting ceramics with the nominal composition $\text{Bi}_{1.6}\text{Pb}_{0.4}\text{Sr}_2\text{Ca}_2\text{Cu}_3\text{O}_{10}$ were synthesised via the co-precipitation method and sintered at temperatures of 845 °C, 850 °C, and 855 °C. X-ray diffraction (XRD) analysis confirmed the dominance of $\text{Bi}_{1.6}\text{Pb}_{0.4}\text{Sr}_2\text{Ca}_2\text{Cu}_3\text{O}_{10}$ phase with minor traces of secondary phases, Ca_2PbO_4 (dicalcium lead (IV) oxide). An increase in sintering temperature led to a larger average grain size and reduced intergranular voids. Electrical resistivity measurements using the four-point probe method revealed the highest superconducting transition temperature ($T_{\text{c onset}} = 104$ K) for samples sintered at 845 °C. Higher sintering temperatures reduced the value of $T_{\text{c onset}}$ and resulted in a wider transition width, ΔT_{c} . These findings highlight the critical influence of sintering temperature on the structural and microstructural properties, which in turn govern the superconducting performance of (Bi, Pb)-2223 ceramics.

Keywords: BSCCO-2223; Co-precipitation; Sintering; Superconducting; Temperature

Introduction

High-temperature superconductors (HTS) are promising materials with potential usages in power transmission, magnetic levitation, energy storage systems, and advanced electronic devices (Hull, 2003; Shimoyama & Motoki, 2024). Among the various HTS families, bismuth-based superconductors, especially $\text{Bi}_2\text{Sr}_2\text{Ca}_2\text{Cu}_3\text{O}_{10+x}$ (Bi-2223) phase, have drawn special interest due to their high critical temperature (T_{c}) above 110 K, good chemical stability, and strong directional behavior (anisotropy). In addition, Bi-2223 can be processed into wires and tapes (Kikuchi et al., 2008; Lei et al., 2023), making it suitable for real-world applications such as high-field magnets and fault

current limiters (Janowski et al., 2004). The synthesis method plays a crucial role in determining the phase formation, grain connectivity, microstructure, and ultimately the superconducting properties of BSCCO materials. The conventional solid-state reaction method is commonly used due to its feasibility (Çetin & Gündoğmuş, 2024; Lojka et al., 2020). However, it has several drawbacks, including uneven grain sizes and phase inhomogeneity in the produced samples, as well as prolonged heat treatments due to poor diffusion and incomplete chemical reactions (Hapipi et al., 2019; Mohiju et al., 2022). Furthermore, it requires multiple grinding and calcination steps to enhance uniformity. To overcome these limitations, alternative synthesis methods such as co-precipitation (COP) have been

How to Cite:

Hapipi, N. M., Chen, S. K., Kechik, M. M. A., Lim, K. P., Shaari, A. H., Baharuddin, N. A., ... Lee, O. J. (2025). Effect of Sintering Temperature on the Phase Formation and Superconducting Properties of $\text{Bi}_{1.6}\text{Pb}_{0.4}\text{Sr}_2\text{Ca}_2\text{Cu}_3\text{O}_{10}$ Ceramics Synthesised via Co-Precipitation. *Journal of Material Science and Radiation*, 1(2), 66–71. Retrieved from <https://journals.balaipublikasi.id/index.php/jmsr/article/view/387>

explored (Abdullah et al., 2023; Hapipi et al., 2019; Mohiju et al., 2022). This method allows better control of the chemical composition and produces fine, uniform powders with higher purity. The particles formed through COP method are much smaller and more consistent in size than those of solid-state reaction method, leading to improved superconducting properties of the materials (Hapipi et al., 2019; Mohiju et al., 2022; Ochsenkühn-Petropulu et al., 1998).

Thermal treatments such as annealing, calcination, and sintering are essential in influencing microstructural evolution, densification, grain growth, and phase development (Fallah-Arani et al., 2017; Mohammed et al., 2012). Annealing helps relieve internal stresses and enhances grain connectivity, while calcination and sintering promote phase formation and crystallinity. Sintering, in particular, facilitates densification and grain growth by applying thermal energy below the melting point, allowing solid-state diffusion without the formation of a liquid phase (William et al., 2009). It has been reported that the phase formation of Bi-2201 starts to occur at temperatures as low as 750 °C and gradually transforms into Bi-2212 phase around 800 °C (Popa et al., 1998). At approximately 850 °C, Bi-2201 is almost fully transformed into Bi-2212, and the Bi-2223 phase starts to appear (Hsueh et al., 2001; Popa et al., 1998). Sintering at temperatures between 835 °C and 855 °C has been found to increase the phase formation of Bi-2223 while reducing the Bi-2212 content (Mohammed et al., 2012). Further increase in temperature up to 865 °C promotes the formation of Bi-2223 phase (Kameli et al., 2006). However, excessively high temperatures may cause the formation of a secondary liquid phase, which disrupts grain connectivity and weakens intergrain coupling, thus reducing the critical current density (J_c) (Kameli et al., 2006).

In this study, Bi-2223 superconductors were synthesised using co-precipitation method, whereby the sintering temperatures were varied between 845 °C and 855 °C to investigate their effect on phase formation, grain morphology, and superconducting behaviours of the material. This study aims to identify the optimal sintering temperatures for improvement of superconducting properties.

Method

Samples with nominal composition $\text{Bi}_{1.6}\text{Pb}_{0.4}\text{Sr}_2\text{Ca}_2\text{Cu}_3\text{O}_x$ were synthesised using co-precipitation (COP) method. High-purity metal acetates of bismuth (III) acetate ($\text{Bi}(\text{CH}_3\text{COO})_3$, 99.9%, Alfa Aesar), lead (II) acetate trihydrate ($\text{Pb}(\text{CH}_3\text{COO})_2 \cdot 3\text{H}_2\text{O}$, 99.9%, Fluka), strontium acetate ($\text{Sr}(\text{CH}_3\text{COO})_2$, 99.9%, Sigma Aldrich), calcium acetate hydrate ($\text{Ca}(\text{CH}_3\text{COO})_2 \cdot \text{H}_2\text{O}$, 99.9%, Fluka), and copper (II) acetate monohydrate ($\text{Cu}(\text{CH}_3\text{COO})_2 \cdot \text{H}_2\text{O}$, 99.9%, Alfa

Aesar) were carefully weighed according to the stoichiometric ratio $\text{Bi: Pb: Sr: Ca: Cu} = 1.6: 0.4: 2.0: 2.0: 3.0$ to ensure the desired chemical composition. Initially, $(\text{Bi}(\text{CH}_3\text{COO})_3$ was preheated at 50 °C for 10 minutes to enhance its solubility. Subsequently, Pb, Sr, Ca, and Cu acetates were mixed in a beaker. Then, 500 mL of glacial acetic acid was added until a dark blue solution was formed (Solution A). Solution A was then stirred at 400 rpm for 2 hours at 80 °C using a magnetic stirrer. At the same time, oxalic acid was dissolved in a mixture of distilled water and 2-propanol (2:3 volume ratio) to form solution B, which was stirred at 400 rpm for 2 hours at room temperature without heating.

After stirring, both solutions were cooled in an ice bath to below 5 °C. To prevent freezing, solution A was continuously stirred manually, while solution B was slowly added to solution A over 10 minutes with continuous magnetic stirring until a uniform blue suspension was obtained. The resulting slurry was filtered using a Büchner funnel, and the precipitate was dried in an oven at 85 °C for 12 hours. The dried powder was then ground manually for one hour using an agate mortar and pestle. The powder was subjected to a two-step calcination process. The first step involved pre-calcination at 730 °C for 12 hours in air to remove residual volatile components. After regrinding, a second calcination was conducted at 845 °C for 24 hours in our attempt to eliminate the Bi-2201 phase (Hamadneh et al., 2006).

The resulting powder was pressed into pellets with a diameter of 13 mm and a thickness of 2 mm, using a hydraulic press at 5 tons of applied pressure for 5 minutes. The pellets were then sintered in air at different temperatures (845 °C, 850 °C, and 855 °C, respectively) for 48 hours to promote grain growth and formation of Bi-2223 phase. The heating and cooling rates were set at 2 °C/min and 1 °C/min, respectively. The crystal structure and phase formation were studied using X-ray diffraction (XRD) using a PW 3040/60 MPD X'Pert Pro Panalytical Philips DY 1861 diffractometer with Cu-K α radiation. Scans were performed over the 2θ range of 20° to 80° with an increment step size of 0.03°. The resulting diffraction patterns were analysed using X'Pert HighScore Plus software. Grain morphology and elemental analysis were carried out using a scanning electron microscopy (SEM-LEO 1455 VP SEM) equipped with an energy dispersive X-ray spectrometer (EDX). Temperature-dependent resistance of the samples was measured using the standard four-point probe method with a closed-cycle helium cryostat.

Results and Discussion

X-ray Diffraction (XRD) Analysis

Figure 1 shows the XRD patterns at different sintering temperatures of 845 °C, 850 °C, and 855 °C. The

results show that the dominant peaks in all samples correspond to the $\text{Bi}_{1.6}\text{Pb}_{0.4}\text{Sr}_2\text{Ca}_2\text{Cu}_3\text{O}_{10}$ ((Bi, Pb)-2223) phase (ICSD: 98-002-5549) with a tetragonal structure (space group I4/mmm), confirming the successful formation of the desired superconducting phase. The secondary phases, dicalcium lead (IV) oxide (Ca_2PbO_4) (ICSD: 98-001-6450), can be observed at $2\theta = 31.0^\circ$, similar to the previous report (Abou-Aly et al., 2011; Hamadneh et al., 2006; Hsueh et al., 2001; Kameli et al., 2006). This phase is known to form during calcination process and plays a transitional role in (Bi, Pb)-2223 formation before diminishing during sintering (Jeremie et al., 1997).

Table 1 shows that the (Bi, Pb)-2223 intensity fraction decreases to 92.7% at 850 °C, compared to 97.1% and 97.3% at 845 °C and 855 °C, respectively. The decreasing (Bi, Pb)-2223 intensity fraction to 92.7% can be attributed to the temperature-dependent stability and slower formation kinetics of the (Bi, Pb)-2223 superconducting phase. However, at 855 °C, the conditions are more favourable for phase formation, leading to a higher intensity fraction of (Bi, Pb)-2223 phase. The intensity fraction of Bi-2223 and Ca_2PbO_4 was estimated by using the equation below (Abou-Aly et al., 2011).

$$\text{Bi-2223 (\%)} \approx \sum I_{2223} / (\sum I_{2223} + \sum I_{\text{Ca}_2\text{PbO}_4}) \times 100 \quad (1)$$

$$\text{Ca}_2\text{PbO}_4 (\%) \approx \sum I_{\text{Ca}_2\text{PbO}_4} / (\sum I_{2223} + \sum I_{\text{Ca}_2\text{PbO}_4}) \times 100 \quad (2)$$

where I is the intensity of the respective phase.

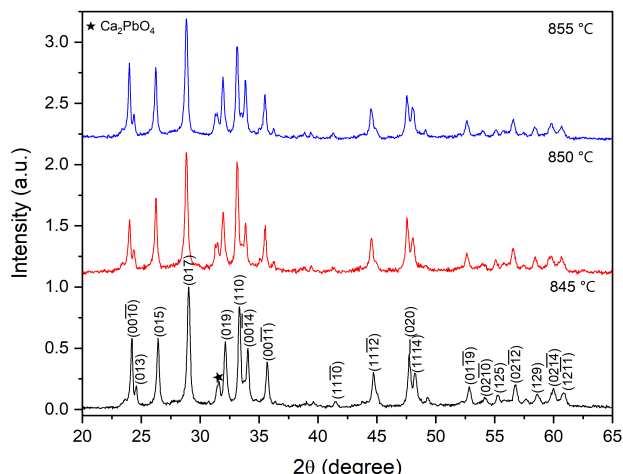


Figure 1. XRD patterns of samples sintered at different temperatures

Table 1. Relative intensity fraction of Bi-2223 and Ca_2PbO_4 phases for all samples

Sintering temp. (°C)	(Bi, Pb)-2223 (%)	Ca_2PbO (%)
845	97.1	2.9
850	92.7	7.3
855	97.3	2.7

Scanning Electron Microscopy (SEM) and Energy Dispersive X-ray (EDX)

Figure 2 shows high magnification scanning electron microscope (SEM) images of fractured surfaces for all samples. All samples display the compacted layers of thin flake-like grains. The intergranular voids (dark regions) can be clearly observed for samples sintered at lower temperature of 845 °C (Figure 2 (a)) and it reduced with increasing sintering temperature. Table 2 shows the average grain size, determined from 50 randomly selected grains based on the SEM images analysed with Image-J software. The results show that the grain size of the samples increased from 4.68 μm to 5.47 μm with increasing sintering temperature from 845 °C to 855 °C. It shows that increasing sintering temperatures promote the grain growth of the samples and improve the grain connectivity of the samples.

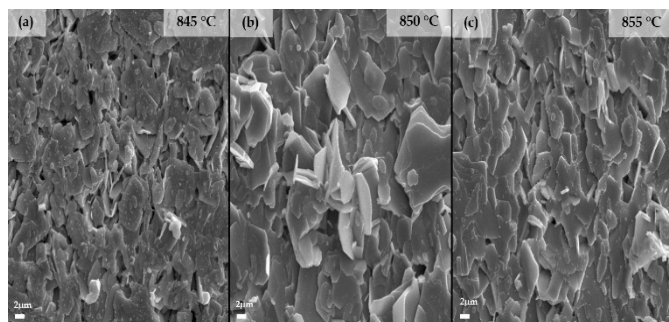


Figure 2. High magnification SEM images of fractured surfaces for (Bi, Pb)-2223 samples sintered at (a) 845 °C, (b) 850 °C, and (c) 855 °C

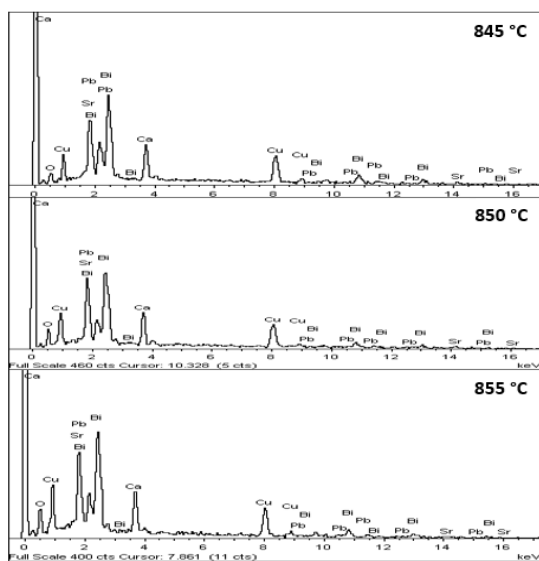
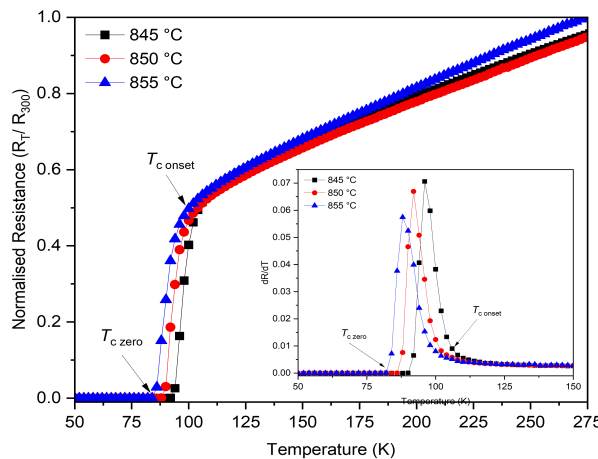
Table 2. Average grain size of (Bi, Pb)-2223 sintered at different temperatures

Sintering temp. (°C)	Average grain size (μm)
845	4.68
850	5.41
855	5.47

To further understand the elemental distribution, energy dispersive X-ray (EDX) analysis was performed on the same regions of the SEM images. Figure 3 shows that all elements Bi, Pb, Sr, Ca, Cu, and O could be detected, ignoring the possibility of any impurities in the sample. Notably, the calcium content decreased at higher sintering temperatures, particularly at 850 °C. This deviation in stoichiometry, as presented in Table 3, supports the XRD results of increased secondary phase formation at 850 °C, as the Ca deficiency likely contributes to the instability of the Bi-2223 phase. EDX results suggest that 845 °C and 855 °C samples achieved a closer approximation to the intended ratio of Bi: Sr: Ca: Cu = 2: 2: 2: 3.

Table 3. Ratio of (Bi, Pb)-2223 sintered at different sintering temperatures

Sintering temp. (°C)	Bi	Sr	Ca	Cu	O	Ratio
845	12.7	12.0	11.8	19.6	43.9	2.0:1.9:1.9:3.1:6.9
850	8.3	9.4	8.3	18.8	55.3	2.0:2.3:2.0:4.5:13.4
855	7.9	7.8	8.7	13.7	60.8	2.0:2.0:2.2:3.5:15.3

**Figure 3.** EDX spectra for (Bi, Pb)-2223 sintered at 845 °C, 850 °C, and 855 °C**Figure 4.** Normalised resistance versus temperature curves for (Bi, Pb)-2223 sintered at 845 °C, 850 °C, and 855 °C. Inset shows the derivative of resistance against temperature

Four-Point Probe (4PP) Measurements

Figure 4 shows the temperature dependence of normalised resistance (R_t/R_{300K}) for the samples measured in the range of 50 K to 275 K. The insets show the derivative plots of resistance to precisely identify the superconducting transition onset temperature (T_c onset) and zero resistance temperature (T_c zero), based on the inflection point of the plots. T_c onset is defined as the temperature at which the materials start to behave as a superconductor, while T_c zero is the temperature at which the resistance becomes zero (Hapipi et al., 2017). All

samples exhibit metallic-like behaviour in the normal state, followed by a sharp transition to zero resistance ($R = 0$) as temperature decreases, confirming the T_c onset of superconductivity (Mohammed et al., 2012). The metallic nature indicates well-connected grains, allowing for electron conduction above the superconducting transition. All samples show a single step transition, implying good grain connectivity and dominance of (Bi, Pb)-2223 (Hamadneh et al., 2008; Hapipi et al., 2017).

Table 4. The properties of superconducting transition temperature, T_c onset, T_c zero and ΔT_c of the samples

Sintering temp.(°C)	T_c onset	T_c zero	ΔT_c (K)
845	104	92	12
850	100	86	14
855	98	82	16

Table 4 shows that the T_c onset values for the samples sintered at 845 °C, 850 °C, and 855 °C are 104 K, 100 K and 98 K, respectively. The highest T_c onset was obtained at 845 °C, which is 104 K. Then, the values of T_c decrease with increasing sintering temperature. Lastly, the width transition, ΔT_c values for each sample, is broadened with increasing sintering temperature, indicating the possibility of degradation of local homogeneity within the samples (Hapipi et al., 2018).

Conclusions

In this study, (Bi, Pb)-2223 superconducting samples were successfully prepared using co-precipitation method by sintering at different temperatures between 845 °C and 855 °C. XRD results confirmed that the main phase in all samples was (Bi, Pb)-2223 with a tetragonal crystal structure. The minor phase of Ca_2PbO_4 can also be observed, particularly at higher sintering temperatures. SEM images showed that higher sintering temperatures improved grain growth and reduced porosity, leading to better grain connectivity. Electrical transport measurements showed the highest critical temperature, T_c onset = 104 K, and the sharpest superconducting transition for sample sintered at 845 °C, making it the best sintering temperature in this study.

Acknowledgments

This research was funded by the Ministry of Higher Education Malaysia through the Fundamental Research Grant Scheme (FRGS/1/2023/STG05/UPM/02/6).

Author Contributions

Conceptualization, N.M.H., S.K.C., and M.M.A.K.; Methodology, N.M.H., S.K.C., N.A.B., N.A.K.; Validation, N.M.H., S.K.C., O.J.L., A.H.S., M.M.A.K., K.P.L., M.K.S., and K.B.T.; Original draft preparation, N.M.H.; Writing-review and editing, S.K.C., M.M.A.K., and O.J.L.; Supervision, S.K.C., M.M.A.K., and K.B.T.; Funding acquisition, S.K.C., O.J.L., A.H.S., M.M.A.K., K.P.L., and M.K.S.

Funding

This research was funded by the Ministry of Higher Education Malaysia through the Fundamental Research Grant Scheme (FRGS/1/2023/STG05/UPM/02/6).

Conflicts of Interest

The authors declare no conflict of interest.

References

Abdullah, S. N., Kechik, M. M. A., Kamarudin, A. N., Talib, Z. A., Baqiah, H., Kien, C. S., Pah, L. K., Abdul Karim, M. K., Shabdin, M. K., Shaari, A. H., Hashim, A., Suhaimi, N. E., & Miryala, M. (2023). Microstructure and Superconducting Properties of Bi-2223 Synthesized via Co-Precipitation Method: Effects of Graphene Nanoparticle Addition. *Nanomaterials*, 13(15). <https://doi.org/10.3390/nano13152197>

Abou-Aly, A. I., Awad, R., Mahmoud, S. A., & Barakat, M. M. (2011). EPR studies of (Bi, Pb)-2223 phase substituted by Ruthenium ions. *Journal of Alloys and Compounds*, 509, 7381-7388. <https://doi.org/10.1016/j.jallcom.2011.03.160>

Çetin, Y., & Gündoğmuş, H. (2024). Investigation of BSCCO superconductors with Ga substitution by solid state method. *Cumhuriyet Science Journal*, 45(2), 407-413. <https://doi.org/10.17776/csj.1429356>

Fallah-Arani, H., Baghshahi, S., Sedghi, A., Stornaiuolo, D., Tafuri, F., Massarotti, D., & Riahi-Noori, N. (2017). The influence of heat treatment on the microstructure, flux pinning and magnetic properties of bulk BSCCO samples prepared by sol-gel route. *Ceramics International*, 44(5), 5209-5218. <https://doi.org/10.1016/j.ceramint.2017.12.128>

Hamadneh, I., Halim, S. A., & Lee, C. K. (2006). Characterization of Bi_{1.6}Pb_{0.4}Sr₂Ca₂Cu₃O_y ceramic superconductor prepared via coprecipitation method at different sintering time. *Journal of Materials Science*, 41, 5526-5530. <https://doi.org/10.1007/s10853-006-0277-3>

Hamadneh, I., Rosli, A. M., Abd-Shukor, R., Suib, N. R. M., & Yahya, S. Y. (2008). Superconductivity of REBa₂Cu₃O_{7-δ} (RE= Y, Dy, Er) ceramic synthesized via coprecipitation method. *Journal of Physics: Conference Series*, 97, 12063. <https://doi.org/10.1088/1742-6596/97/1/012063>

Hapipi, N. M., Chen, S. K., Shaari, A. H., Kechik, M. M. A., Tan, K. B., & Lim, K. P. (2018). Superconductivity of Y₂O₃ and BaZrO₃ nanoparticles co-added YBa₂Cu₃O_{7-δ} bulks prepared using co-precipitation method. *Journal of Materials Science: Materials in Electronics*, 29, 18684-18692. <https://doi.org/10.1007/s10854-018-9991-2>

Hapipi, N. M., Lim, J. K., Chen, S. K., Lee, O. J., Shaari, A. H., Kechik, M. M. A., Lim, K. P., Tan, K. B., Murakami, M., & Miryala, M. (2019). Comparative study on ac susceptibility of YBa₂Cu₃O_{7-δ} added with BaZrO₃ nanoparticles prepared via solid-state and co-precipitation method. *Crystals*, 9, 1-12. <https://doi.org/10.3390/crust9100497>

Hapipi, N. M., Shaari, A. H., Kechik, M. M. A., Tan, K. B., Abd-Shukor, R., Mohd Suib, N. R., & Chen, S. K. (2017). Effect of heat treatment condition on the phase formation of YBa₂Cu₃O_{7-δ} superconductor. *Solid State Phenom*, 268, 305-310. Retrieved from <https://www.scientific.net/ssp.268.305>

Hsueh, Y. W., Chang, S. C., Liu, R. S., Woodall, L., & Gerards, M. (2001). A comparison of the properties of Bi-2223 precursor powders synthesized by various methods. *Materials Research Bulletin*, 36, 1653-1658. [https://doi.org/10.1016/S0025-5408\(01\)00647-X](https://doi.org/10.1016/S0025-5408(01)00647-X)

Hull, J. R. (2003). Applications of high-temperature superconductors in power technology. *Reports on Progress in Physics*, 66, 1865-1886. <https://doi.org/10.1088/0034-4885/66/11/R01>

Janowski, T., Stryczewska, H. D., Kozak, S., Kondratowicz-Kucewicz, B., Wojtasiewicz, G., Kozak, J., Surdacki, P., & Malinowski, H. (2004). Bi-2223 and Bi-2212 tubes for small fault current limiters. *IEEE transactions on applied superconductivity*, 14, 851-854. <https://doi.org/10.1109/TASC.2004.830298>

Jeremie, A., Grasso, G., & Flükiger, R. (1997). Synthesis and characterization of high temperature superconductors: System Bi-Pb-Sr-Ca-Cu-O. *Journal of Thermal Analysis*, 48, 3. <https://doi.org/10.1007/BF01979509>

Kameli, P., Salamati, H., & Eslami, M. (2006). The effect of sintering temperature on the intergranular properties of Bi2223 superconductors. *Solid State Commun*, 137(1-2), 30-35. <https://doi.org/10.1016/j.ssc.2005.10.026>

Kikuchi, M., Ayai, N., Ishida, T., Tatamidani, K., Hayashi, K., Kobayashi, S., Ueno, E., Yamazaki, K., Yamade, S., Takaaze, H., Fujikami, J., & Sato, K. I. (2008). Development of new types of DI-BSCCO wire. *SEI TECHNICAL REVIEW-ENGLISH EDITION*, 66, 73-80. Retrieved from <https://global-sei.com/technology/tr/bn66/pdf/66-09.pdf>

Lei, Z., Yao, C., Guo, W., Wang, D., & Ma, Y. (2023).

Progress on the fabrication of superconducting wires and tapes via hot isostatic pressing. *Materials*, 16, 1786. <https://doi.org/10.3390/ma16051786>

Lojka, M., Antoncik, F., Sedmidubsky, D., Hlasek, T., Wild, J., Pavlu, J., Jankovsky, O., & Bartunek, V. (2020). Phase-stable segmentation of BSCCO high-temperature superconductor into micro-, meso-, and nano-size fractions. *Journal of Materials Research and Technology*, 9, 12071-12079. <https://doi.org/10.1016/j.jmrt.2020.08.107>

Mohammed, N. H., Awad, R., Abou-Aly, A. I., Ibrahim, I. H., & Hassan, M. S. (2012). Optimizing the preparation conditions of Bi-2223 superconducting phase using PbO and PbO₂. *Materials Sciences and Applications*, 3, 224-233. <https://doi.org/10.4236/msa.2012.34033>

Mohiju, Z. A., Mujaini, M., & Hamid, N. A. (2022). Superconducting properties of (Bi, Pb)2Sr2Ca2Cu3O_x (BSCCO-2223) superconductor ceramics prepared by conventional solid-state reaction and co-precipitation methods. *IOP Conference Series: Materials Science and Engineering*, 1231(1). <https://doi.org/10.1088/1757-899X/1231/1/012009>

Ochsenkühn-Petropulu, M., Tarantilis, P., Argyropulu, R., & Parissakis, G. (1998). Optimization of the sintering process by DSC for the preparation of high-temperature superconductors. *J. Therm. Anal.*, 52, 903-914. <https://doi.org/10.1023/A:1010159918410>

Popa, M., Totovkg, A., Popescu, L., & Zaharesc, M. (1998). Reactivity of the Bi, Sr, Ca, Cu oxalate powders used in BSCCO preparation. *Journal of the European Ceramic Society*, 18, 1265-1271. [https://doi.org/10.1016/S0955-2219\(98\)00052-1](https://doi.org/10.1016/S0955-2219(98)00052-1)

Shimoyama, J., & Motoki, T. (2024). Current status of high temperature superconducting materials and their various applications. *IEEJ Transactions on Electrical and Electronic Engineering*, 19, 292-304. <https://doi.org/10.1002/tee.23976>

William, J., Callister, D., & Rethwisch, D. G. (2009). *Materials science and engineering: an introduction*. John Wiley & Sons, Inc.